

Dislocation kink migration energies and the Frenkel-Kontorowa model

B. Joós*

Department of Physics, University of Ottawa, 150 Louis Pasteur, Ottawa, Ontario, Canada K1N 6N5

M. S. Duesbery†

Fairfax Materials Research Inc., 7305 Beechwood Drive, Springfield, Virginia 22153-2336

(Received 21 October 1996)

An analytic solution of the Peierls pinning energy E_p in the discrete Frenkel-Kontorowa (FK) model is used to obtain estimates of the second-order Peierls stress σ_{2P} controlling dislocation kink motion. From the Dorn-Rajnak model the kink migration energy is shown to be the Peierls pinning energy E_p in the FK model. The required parameters are related to features of the generalized stacking fault surface. Examples illustrate use of the approach. [S0163-1829(97)12317-7]

I. INTRODUCTION

Modern structural (intermetallics, metal silicides) and electronic (silicon, GaAs, CdTe) materials are complex and not readily amenable to the atomistic methods which have been so successful in their description of simpler materials. Although increasingly sophisticated quantum mechanical techniques are currently being developed by a number of workers, there is an immediate need for a rapid, low-cost, and reliable means to estimate the fundamental mechanical properties of these complex materials. In particular, methods which link the quantum mechanical capabilities of modern physics to the continuum mechanical scale are needed.

In recent work the authors have demonstrated, using silicon as an example, that these means are available in some measure for dislocations. For example, it was shown that the Peierls-Nabarro (PN) model^{1,2} used with a generalized stacking fault energy surface³ calculated from first principles⁴ can predict a Peierls stress which is in good agreement with the values obtained from atomistic computations.⁵⁻⁷ The PN-based Dorn-Rajnak (DR) kink pair formalism⁸ was shown to provide an explanation for the unexpected preference in silicon for slip on the glide, rather than shuffle planes, and to predict an activation enthalpy for kink pair nucleation in agreement with experiment.⁹

II. KINKS IN DISLOCATIONS

In materials with significant Peierls stress, dislocations do not move by rigid translation, but rather by the nucleation and propagation of kink pairs. A kink pair is created when part of the dislocation line is activated to a neighboring low energy channel (see Fig. 1). The energy barrier to be overcome is called the PN energy W_{PN} . As is well known,¹⁰ the kink pair mechanism for dislocation motion admits two limiting cases. At high stresses, the rate-controlling mechanism is the nucleation of kink pairs. At low stresses, the periodic potential through which an individual kink must move may be large enough to control the process; this is referred to as the kink migration regime and its resistive stress at 0 K, σ_{2P} , is commonly termed the second-order Peierls stress.

This paper will show that σ_{2P} can be estimated for com-

plex materials by a simple extension of the PN-DR models, provided only that the appropriate cross section of the generalized stacking fault (gsf) energy surface is known.

Let us return to Fig. 1, which shows a kinked dislocation with Burgers vector \vec{b} in a material with high W_{PN} . The low energy dislocation line channels are chosen to lie parallel to the x axis and are separated by $y=h$. The shape of the kink is then described by $y(x)$, with $y(-\infty)=0$ and $y(\infty)=h$. W_{PN} is periodic in y with period h . The DR formalism makes the assumption that the dislocation line energy $\Gamma(y)$ is a simple sum of the intrinsic (unperturbed) line energy Γ_0 and the PN energy, that is

$$\Gamma(y) = \Gamma_0 + W_{PN}(y). \quad (1)$$

Equation (1) leads to the following Hamiltonian for the DR kink:

$$H = \int_{-\infty}^{\infty} \left[\Gamma(y) \left\{ 1 + \left(\frac{dy}{dx} \right)^2 \right\}^{1/2} - \Gamma_0 \right] dx. \quad (2)$$

In the limit $dy/dx \ll 1$, Eq. (2) can be rewritten as

$$H = \frac{1}{2} \Gamma_0 \int_{-\infty}^{\infty} \left(\frac{dy}{dx} \right)^2 dx + \int_{-\infty}^{\infty} W_{PN}[y(x)] dx. \quad (3)$$

This Hamiltonian can be viewed as a functional of the distinct variables, $y(x)$ and $y' = dy/dx$:

$$H = \int_{-\infty}^{\infty} F\{y(x), y'(x); x\} dx. \quad (4)$$

Euler's equation,

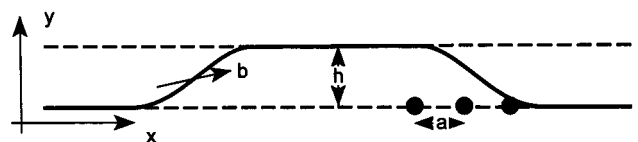


FIG. 1. A kink pair in a dislocation.

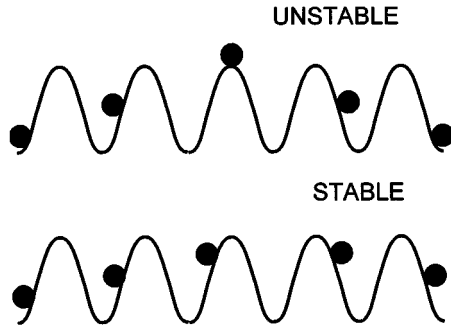


FIG. 2. Stable and unstable soliton configurations.

$$\frac{\partial F}{\partial y} - \frac{d}{dx} \frac{\partial F}{\partial y'} = 0, \quad (5)$$

determines the kink shape $y(x)$ which minimizes H . This can be written as

$$\Gamma_0 \frac{d^2 y}{dx^2} = \frac{dW_{\text{PN}}}{dy}. \quad (6)$$

Multiplying both sides of Eq. (6) by dy/dx and integrating yields the equation

$$\frac{\Gamma_0}{2} \left(\frac{dy}{dx} \right)^2 = W_{\text{PN}}(y), \quad (7)$$

which shows that the approximation $dy/dx \ll 1$ is equivalent to requiring that $W_{\text{PN}}/\Gamma_0 \ll 1$.

Equations (2)–(7) describe a continuous mass kink, the energy of which is invariant to translation along the dislocation line. In order to determine the mobility of the kink in a crystal lattice, the discreteness of the lattice must be restored by converting Eq. (3) into a sum over atomic sites. If at the same time we set $y = \zeta h$, and $x = na$, where n is an integer and a is the repeat distance of atomic planes along the dislocation line (see Fig. 1), the discretized Hamiltonian becomes

$$\frac{H}{(\Gamma_0 h^2/a)} = \frac{1}{2} \sum_{n=-\infty}^{\infty} \left(\frac{d\zeta}{dn} \right)^2 + \frac{a^2}{\Gamma_0 h^2} \sum_{n=-\infty}^{\infty} W_{\text{PN}}[h\zeta(n)]. \quad (8)$$

As is known,¹¹ when the PN energy is sinusoidal, Eq. (8) is identical with the Hamiltonian of the Frenkel-Kontorowa (FK) model,^{12,13} and Eq. (6) reduces to the sine-Gordon equation.

III. THE FRENKEL-KONTOROWA MODEL

The Frenkel-Kontorowa (FK) model^{12,13} is perhaps the simplest model of a dislocation, consisting of a string of atoms connected by springs and subjected to a periodic sinusoidal potential (see Fig. 2). It is also representative of solitons or domain walls in one- and two-dimensional lattices.^{14,15} An accurate analytic solution is available for the key quantity, the pinning potential of the solitonlike defects in the chain. This energy, known as the Peierls potential E_p ,^{16,17} is calculated here by assuming that, as it moves in the lattice, the soliton profile remains undeformed. The solu-

tions for narrow and wide solitons are in excellent agreement with numerical results for relaxed-profile solitons,^{16,17} demonstrating the validity of the assumption of a rigid dislocation profile.

The classical Hamiltonian for the FK model is

$$H = \frac{\kappa}{2} \sum_{n=-\infty}^{\infty} (y_{n+1} - y_n)^2 + \sum_{n=-\infty}^{\infty} W'(y_n), \quad (9)$$

where y_n is the displacement of the n th particle and κ is the spring constant of the interparticle interaction. W' is the periodic potential, which in the classic FK model is sinusoidal with amplitude W_0 and period h , as

$$W'(y) = \frac{W_0}{2} \left(1 - \cos \frac{2\pi y}{h} \right), \quad (10)$$

where h , the period of the substrate energy, is the Burgers vector of the FK kink. Equations (9) and (10) can be combined and rewritten as

$$\frac{H}{\kappa h^2} = \frac{1}{2} \sum_{n=-\infty}^{\infty} (\zeta_{n+1} - \zeta_n)^2 + \frac{1}{4\lambda^2} \sum_{n=-\infty}^{\infty} (1 - \cos 2\pi \zeta_n), \quad (11)$$

where we define $\zeta_n = y_n/h$ and

$$\lambda = \left(\frac{\kappa h^2}{2W_0} \right)^{1/2}. \quad (12)$$

This dimensionless parameter measures the relative strength of the springs and the periodic restoring forces. The equilibrium configurations of the chain are obtained by solving for the set of difference equations

$$\zeta_{n+1} - 2\zeta_n + \zeta_{n-1} = \frac{\pi}{2\lambda^2} \sin 2\pi \zeta_n. \quad (13)$$

If the variation of ζ_n from particle to particle is small, Eq. (13) can be replaced by the familiar sine-Gordon equation,

$$\frac{d^2 \zeta}{dn^2} = \frac{\pi}{2\lambda^2} \sin 2\pi \zeta. \quad (14)$$

Equations (6) and (14) are identical, as are Eqs. (8) and (11), provided that the PN energy W_{PN} is sinusoidal. All we need to do is substitute κ with Γ_0/a , and W_0 by aW_0 , where W_0 is the amplitude of the PN energy, so that

$$\lambda = \left(\frac{\Gamma_0 h^2}{2W_0 a^2} \right)^{1/2}. \quad (15)$$

The one-soliton solution to Eq. (14) is

$$\zeta(n - \alpha) = \frac{2}{\pi} \tan^{-1} e^{\pi(n - \alpha)/\lambda}, \quad (16)$$

where α is the location of the center of the soliton. The displacement ζ is 0 for $(n - \alpha) = -\infty$, $\frac{1}{2}$ at $(n - \alpha) = \alpha$, and 1 for $(n - \alpha) = +\infty$. From this equation it is clear that λ is the width of the domain wall, or soliton, in the chain measured in units of particle number. λ therefore measures the number of atomic planes over which the kink spreads along the x direction, so its width is given by λa .

IV. THE PEIERLS PINNING POTENTIAL

Equation (16) defines a continuous mass soliton with no Peierls pinning potential. To obtain E_p we have to restore discreteness to the chain. We first assume that, in an actual domain wall, the particle displacements follow the profile (16), which actually has been observed to be true to fairly good accuracy (see, for instance, Ref. 18). We make this assumption not only for the equilibrium stable position, but also for the soliton displaced by α . E_p is obtained from the energy difference between the stable minimum energy configuration ($\alpha=1/2$) and the maximum energy saddle point configuration ($\alpha=0$). The two configurations are shown in Fig. 2.

We calculate the energy variation of the domain wall in two steps. We first consider the contribution of the periodic potential W_{per} , and then the elastic energy in the chain W_{elas} , both expressed in units of κb^2 .

(i) *The periodic potential contribution* to the chain energy is

$$W_{\text{per}} = \frac{1}{4\lambda^2} \sum_{n=-\infty}^{\infty} (1 - \cos 2\pi\zeta_n). \quad (17)$$

Substituting Eq. (16), we get

$$W_{\text{per}}(\alpha) = \frac{1}{4\lambda^2} \sum_{n=-\infty}^{\infty} \{1 - \cos[4 \tan^{-1} e^{\pi(n-\alpha)/\lambda}]\}. \quad (18)$$

Using the identities $\cos^2 y = 1/(1 + \tan^2 y)$, and $\cos 4y = 8\cos^4 y - 8\cos^2 y + 1$, Eq. (18) can be rewritten as

$$W_{\text{per}}(\alpha) = \frac{1}{2\lambda^2} \sum_{n=-\infty}^{\infty} \frac{1}{\cosh^2 \pi(n-\alpha)/\lambda}. \quad (19)$$

This is an even function of period unity, which has a Fourier series of the form

$$W_{\text{per}}(\alpha) = \frac{a_0}{2} + \sum_{m=1}^{\infty} a_m \cos 2\pi m \alpha, \quad (20)$$

where

$$a_m = 2 \int_0^1 \sum_{n=-\infty}^{+\infty} \frac{1}{2l^2} \frac{1}{\cosh^2 \pi(n-\alpha)/\lambda} \cos(2\pi m \alpha) d\alpha. \quad (21)$$

With the change of variable $t = \alpha - n$, this becomes

$$a_m = \frac{1}{\lambda^2} \int_{-\infty}^{+\infty} \frac{\cos 2\pi m t}{\cosh^2 \pi t/\lambda} dt, \quad (22)$$

yielding the following Fourier series:

$$W_{\text{per}}(\alpha) = \frac{1}{\lambda \pi} + \sum_{m=1}^{\infty} \frac{2m}{\sinh \pi m \lambda} \cos 2\pi m \alpha. \quad (23)$$

(ii) *The elastic energy in the chain* is given by

$$W_{\text{elas}} = \frac{1}{2} \sum_{n=-\infty}^{\infty} (\zeta_{n+1} - \zeta_n)^2. \quad (24)$$

If we assume that $(\zeta_{n+1} - \zeta_n)$ can be replaced by the leading term in the Taylor expansion of ζ_n , which is what is done in the DR model,

$$W_{\text{elas}} = \frac{1}{2} \sum_{n=-\infty}^{\infty} \left(\frac{d\zeta_n}{dn} \right)^2. \quad (25)$$

Integration of Eq. (16) gives

$$\left(\frac{d\zeta_n}{dn} \right)^2 = \frac{1}{2\lambda^2} (1 - \cos 2\pi\zeta_n), \quad (26)$$

and hence $W_{\text{elas}} = W_{\text{per}}$, given in Eq. (17), or, within this approximation the total energy of the soliton $W_T(\alpha) = W_{\text{elas}}(\alpha) + W_{\text{per}}(\alpha)$ is given by

$$W_T(\alpha) = \frac{2}{\lambda \pi} + \sum_{m=1}^{\infty} \frac{4m}{\sinh \pi m \lambda} \cos 2\pi m \alpha. \quad (27)$$

We see that the average energy of the soliton is $2/(\lambda \pi)$, the known continuum approximation value.¹³

The Peierls pinning potential E_p is the difference between the maximum and minimum energy configurations, so we have

$$E_p = 8 \sum_{m \text{ odd}}^{\infty} \frac{m}{\sinh \pi m \lambda}. \quad (28)$$

This is a very rapidly converging series. Keeping only the leading term, which itself can be simplified, we find that

$$E_p = 16e^{-\pi\lambda}. \quad (29)$$

The same exponential factor has been obtained previously by different means.^{19,20} The predictions of Eq. (29) can be compared with a numerical calculation which has allowed relaxation of the chain as it is placed in the two configurations shown in Fig. 1.¹⁷ As Table I shows, the agreement is good (correct order of magnitude) already for $\lambda=2$, and convergence is rapid. In the same spirit, the second-order Peierls stress can be estimated to leading order, accurate to about 10%. This gives, recalling that the units used since Eq. (11) for the energy are κh^2 , or $\Gamma_0 h^2/a$,

$$\sigma_{2p} = \frac{1}{h^2} \left(\frac{\partial W_T}{\partial \alpha} \right)_{\max} = 16\pi e^{-\pi\lambda} \kappa. \quad (30)$$

Interestingly this model predicts the same functional dependence of stress on width as does the Peierls-Nabarro model.²¹

For very narrow kinks ($\lambda \leq 1$), E_p can be calculated using the observation that only a few particles will contribute to either W_{per} or W_{elas} . From Eq. (19), the leading contribution to E_p from W_{per} will be

$$W_{\text{per}}(0) = \frac{1}{2\lambda^2} \frac{1}{\cosh^2 0} = \frac{1}{2\lambda^2}. \quad (31)$$

To get the contribution from W_{elas} , we start from Eq. (24), substitute Eq. (16), and use the identity $\tan^{-1} x - \tan^{-1} y = \tan^{-1}(x-y)/(1+xy)$, valid for $xy > -1$, to obtain

TABLE I. Comparison of Peierls pinning potential values from numerical relaxation calculations (columns 2 and 6, from Ref. 17) with the predictions of Eq. (35) (column 3) and Eq. (29) (columns 4 and 7), all in units of κh^2 [for the Frenkel-Kontorowa (FK) model] or $\Gamma_0 h^2/a$ (for the kink model).

λ	E_p	$1/(2\lambda^2) - 1/4$	$16\exp(-\pi\lambda)$	λ	E_p	$16\exp(-\pi\lambda)$
0.5	1.76756	1.7500	3.33	6.0	0.95528×10^{-7}	1.042×10^{-7}
1.0	0.30810	0.2500	0.691	7.0	0.42462×10^{-8}	0.450×10^{-8}
1.5	0.75965×10^{-1}	-	1.44×10^{-1}	8.0	0.18748×10^{-9}	0.195×10^{-9}
2.0	0.18898×10^{-1}	-	0.299×10^{-1}	9.0	0.82391×10^{-11}	0.841×10^{-11}
2.5	0.44179×10^{-2}	-	0.621×10^{-2}	10.0	0.36096×10^{-12}	0.363×10^{-12}
3.0	0.98679×10^{-3}	-	1.291×10^{-3}	11.0	0.15807×10^{-13}	0.157×10^{-13}
4.0	0.46564×10^{-4}	-	0.558×10^{-3}	12.0	0.722×10^{-15}	0.680×10^{-15}
5.0	0.21271×10^{-5}	-	0.241×10^{-5}			

$$W_{\text{elas}}(\alpha) = \frac{2}{\pi^2} \sum_{n=-\infty}^{+\infty} \left[\tan^{-1} \frac{\sinh(\pi/2\lambda)}{\cosh(\pi/2\lambda)[1+2(n-\alpha)]} \right]^2. \quad (32)$$

For the unstable configuration ($\alpha=0$), in the limit $\lambda \rightarrow 0$, two terms will contribute significantly and equally, $n=0$ and $n=-1$, to yield

$$W_{\text{elas}}(0) = 2 \left(\frac{2}{\pi^2} \right) \left(\tan^{-1} \tanh \frac{\pi}{2\lambda} \right)^2 \approx \frac{1}{4}. \quad (33)$$

For the stable configuration ($\alpha=1/2$), in the same limit, only one term will contribute significantly, $n=0$, corresponding to the main stretched bond straddling the soliton core:

$$W_{\text{elas}}\left(\frac{1}{2}\right) = \frac{2}{\pi^2} \left(\tan^{-1} \sinh \frac{\pi}{2\lambda} \right)^2 \approx \frac{1}{2}. \quad (34)$$

Or, the Peierls pinning potential E_p is given by

$$E_p = \frac{1}{2\lambda^2} - \frac{1}{4}, \quad (35)$$

again in agreement with the numerical results of Ref. 17 as seen in Table I.

We can conclude from the above results that the Peierls potentials obtained with the assumptions of a rigid kink profile are in good agreement for all widths with the relaxation results. Equations (29) and (30) are expected to give good results for $\lambda > 2$. In these formulas the relative displacement

of two neighboring particles is replaced by the first term in the Taylor series of the displacement.

This derivation neglects the entropic effects which are part of the thermodynamic free energy. Calculation of the entropy would require a knowledge of the vibrational modes in the stable and unstable configurations. The vibrational modes of the FK kinks have been studied earlier.^{22,23} The entropy could then be obtained by an application of the transition-state theory of Vineyard,²⁴ as has been done recently on related defects.^{4,25}

V. APPLICATION TO KINK MIGRATION

In this section we examine the application of the FK model to kink migration. For the line energy Γ_0 of the dislocations we will approximate the elastic expression for the self-energy of a dislocation $Jb^2 \ln(R/b)$ (where R is the screening length) with the conventional value of $Jb^2/2$ for metals. For silicon, which has a much lower dislocation density and therefore a much larger screening length, we adopt the value of Jb^2 for the line energy.⁹ For most purposes, we shall retain the assumption of the FK model that the PN energy is sinusoidal. λ , the kink width, is then given by Eq. (15), the kink migration energies E_M from Table I. For $\lambda > 2$, E_M and the second-order PS σ_{2P} are given, respectively, by Eqs. (29) and (30).

We apply first the FK model to kinks in silicon, for which the γ surface is known,⁴ and therefore a realistic PN energy can be calculated.⁵ In addition, comparative atomistic work

TABLE II. The kink migration energies E_M and second-order Peierls stresses σ_{2P} for selected kinks in glide and shuffle dislocations in silicon, with a dislocation line along $\langle 110 \rangle$ (see Sec. V). Shown in order of appearance are the Peierls energies W_0 , obtained from the appropriate γ surface section (Refs. 4 and 5); J , the anisotropic elastic dislocation energy factors; b , the Burgers vectors; h , distances between equivalent dislocation line channels; a , distances between glide planes intersecting the dislocation line; Γ_0 , dislocation line energies, equal in this case to Jb^2 (Ref. 9); λ , kink widths given by Eq. (15); E_{nuc} , the kink pair nucleation energies from Ref. 9; E_M , the kink migration energy; the first-order Peierls stresses σ_{1P} from the PN model from Ref. 5; and the second-order Peierls stresses σ_{2P} .

	W_0 (eV \AA^{-1})	J (eV \AA^{-3})	b (\AA)	h (\AA)	a (\AA)	Γ_0 (eV \AA^{-1})	λ	E_{nuc} (eV)	E_M (eV)	σ_{1P} (J)	σ_{2P} (J)
30° glide partial	0.343	0.433	2.22	3.33	3.84	2.13	1.53	2.10	0.628	0.561	0.471
90° glide partial	0.323	0.536	2.22	3.33	3.84	2.64	1.75	-	0.509	0.450	0.358
Shuffle screw	0.148	0.400	3.84	3.33	3.84	5.90	3.87	2.39	1.43×10^{-3}	0.103	3.05×10^{-4}
Shuffle 60°	0.116	0.501	3.84	3.33	3.84	7.39	4.89	-	7.27×10^{-5}	0.076	1.55×10^{-6}

TABLE III. The kink migration energies E_M and second-order Peierls stresses σ_{2P} for kinks in $\langle 100 \rangle$ $\{110\}$ dislocations in $B2$ NiAl. The quantities shown are the same as in Table II, but in this case Peierls energies W_0 , first-order Peierls stresses σ_{1P} , and kink pair nucleation energies E_{nuc} are taken from Ref. 35, and $\Gamma_0 = Jb^2/2$; and E_M and σ_{2P} are from Eqs. (29) and (30), respectively.

	W_0 (eV \AA^{-1})	J (eV \AA^{-3})	b (\AA)	h (\AA)	a (\AA)	Γ_0 (eV \AA^{-1})	λ	E_{nuc} (eV)	E_M (eV)	σ_{1P} (J)	σ_{2P} (J)
$\langle 100 \rangle$ line	0.013	0.064	2.88	4.07	2.88	0.27	4.55	1.56	1.0×10^{-5}	0.161	3.1×10^{-5}
$\langle 110 \rangle$ line	0.013	0.050	2.88	2.88	4.07	0.21	2.00	0.87	0.03	0.280	5.9×10^{-2}
$\langle 111 \rangle$ line	0.0087	0.045	2.88	2.35	2.49	0.19	3.09	0.63	1.10×10^{-3}	0.251	3.2×10^{-3}

is available.⁶ Silicon is also of particular interest because it is the simplest directionally bonded material, and because there is extensive experimental information on its deformation properties. The results are shown in Table II. For completeness, the Peierls energies W_0 and first-order Peierls stresses σ_{1P} from Ref. 5 and the kink pair nucleation energies E_{nuc} from Ref. 9 are also included. λ for the glide partials is smaller than two. The predictions of Eqs. (29) and (30) for E_M and σ_{2P} , respectively, are therefore not the values to retain for these dislocations. Focusing, in this discussion, on the 30° partial with the smallest $\lambda = 1.53$ (similar results apply to the 90° partial), we see, comparing columns 2 and 4 in Table I, that corrections of the order of a factor of 2 apply, reducing E_M from 0.804 eV to 0.430 eV. There is a similar effect for σ_{2P} , obtained by applying stress to the relaxed kinks until they move. σ_{2P} is found to decrease from $0.514J$ to $0.27J$. There is another source of correction to consider, which in large part compensates for these decreases, the departure of the PN energy from a sinusoidal function. The impact of this change on the solutions for kink profiles in the FK model has been discussed by Peyrard and Remoissenet.²⁶ Repeating our calculations with their kink solutions, and including relaxation, we find that the deviations, which are present in silicon, cause E_M and σ_{2P} for the 30° partial to increase (from the relaxed sinusoidal case) to 0.628 eV and $0.471J$, respectively. We intend to give more details on the effects of these approximations in a future publication.

The atomistic work of Bulatov, Yip, and Argon,²⁷ using an empirical potential model of Si, yields very similar values for the E_M of the 30° glide partial; 0.74 eV for the right kink, and 0.82 eV for the left kink. Considering that the gsF surface obtained in the Stillinger-Weber potential model of Si used in Ref. 27 has for the relevant $\langle 211 \rangle$ direction, a maximum noticeably larger than in the corresponding local-density approximation (LDA) result,²⁸ we have good agreement between the two predictions.

Measurements indicate that the activation enthalpy for dislocation motion in silicon is about 2.2 eV.²⁹ Conventional thinking is that the kink migration energy may be responsible for as much as a half of this figure, 1.1–1.2 eV.^{30,31} The values in Table II are consistent with the total activation energy for glide, bearing in mind that the calculation takes into account only the most important features of the mechanical aspects of kink migration, and does not consider possible electromechanical interaction terms. Our migration energies represent about a third of the nucleation energies for glide set dislocations, instead of a half as usually assumed.

The migration energies are negligible for shuffle set dislocations. The small values for these kinks are due to the large Burgers vector, which makes the dislocation stiffer and the kink wider.

Second, we consider kink migration in $B2$ ordered NiAl. In contrast with covalent materials, the kink migration energy in metals is expected to be small (Schottky, using a semiempirical elastic calculation, estimates a migration energy of order 0.5 K;³² Duesbery, with an atomistic model, finds a migration stress of less than $10^{-7}\mu$ in potassium³³). The γ surface for NiAl has been calculated from first principles³⁴ and PN-DR model results are available.³⁵ Dislocations with the Burgers vector $\langle 100 \rangle$ lying in $\{110\}$ planes are responsible for plastic deformation except for some restricted orientations of the applied stress. For reasons which are not clearly understood, most observed dislocations have mixed character, with $\langle 111 \rangle$ line directions rather than the $\langle 100 \rangle$ screw or $\langle 110 \rangle$ edge directions. We have calculated for these dislocations the kink widths λ and migration energies E_M , and the second order Peierls stresses σ_{2P} . These are shown in Table III, along with the PN energies W_0 , the kink nucleation energies E_{nuc} , and the first-order Peierls stresses σ_{1P} from Ref. 35. It is clear from Table III that, although the $\langle 100 \rangle$ screw dislocation has the smallest first- and second-order Peierls stresses, the $\langle 110 \rangle$ edge and $\langle 111 \rangle$ mixed dislocations have much smaller kink pair nucleation energies, and of these latter two the $\langle 111 \rangle$ mixed dislocation has a much smaller second-order Peierls stress.

VI. SUMMARY AND CONCLUSIONS

Recent work by the authors on the estimation of dislocation properties in complex materials by the use of approximate mechanical models combined with first-principles generalized stacking fault energy surfaces has been extended to cover the calculation of dislocation kink migration energies and stresses. The results are compatible with experimental work on silicon and explain unusual features of plastic deformation in NiAl.

ACKNOWLEDGMENTS

This work was funded by the Natural Sciences and Engineering Research Council (Canada) and by the Office of Naval Research under SBIR Contract No. N00014-95-C-0404.

- *Electronic address: joos@physics.uottawa.ca
†Electronic address: duesbery@aol.com
- ¹R. Peierls, Proc. Phys. Soc. London **52**, 34 (1940).
 - ²F.R.N. Nabarro, Proc. Phys. Soc. London **59**, 256 (1947).
 - ³V. Vitek, Philos. Mag. **18**, 773 (1968).
 - ⁴E. Kaxiras and M.S. Duesbery, Phys. Rev. Lett. **70**, 3752 (1993).
 - ⁵B. Joós, Q. Ren, and M.S. Duesbery, Phys. Rev. B **50**, 5890 (1994); **53**, 11 882(E) (1996).
 - ⁶Q. Ren, B. Joós, and M.S. Duesbery, Phys. Rev. B **52**, 13 223 (1995); **53**, 11 883(E) (1996).
 - ⁷L.B. Hansen, K. Stokbro, B.I. Lundqvist, K.W. Jacobsen, and D.M. Deaven, Phys. Rev. Lett. **75**, 4444 (1995).
 - ⁸J.E. Dorn and S. Rajnak, Trans. AIME **230**, 1052 (1964); P. Guyot and J.E. Dorn, Can. J. Phys. **45**, 983 (1967).
 - ⁹M.S. Duesbery and B. Joós, Philos. Mag. Lett. **74**, 253 (1996).
 - ¹⁰J.P. Hirth and J. Lothe, *Theory of Dislocations*, 2nd ed. (Wiley, New York, 1982), p. 376.
 - ¹¹A. Seeger and P. Schiller, Acta Metall. **10**, 348 (1962).
 - ¹²J. Frenkel and T. Kontorowa, Phys. Z. Sowjet **13**, 1 (1938).
 - ¹³F.C. Frank and J.H. van der Merwe, Proc. R. Soc. London A **198**, 205 (1949).
 - ¹⁴V.L. Pokrovsky and A.L. Talapov, *Theory of Incommensurate Crystals* (Harwood Academic, New York, 1984).
 - ¹⁵B. Joós, in *Dislocations in Solids*, edited by F.R.N. Nabarro and M.S. Duesbery (Elsevier, Amsterdam, 1996), Vol. 10, p. 505.
 - ¹⁶R. Hobart, J. Appl. Phys. **36**, 1944 (1965).
 - ¹⁷B. Joós, Solid State Commun. **42**, 709 (1982).
 - ¹⁸R.J. Gooding, B. Joós, and B. Bergersen, Phys. Rev. B **27**, 7669 (1983); M.B. Gordon and F. Lançon, J. Phys. C **18**, 3929 (1985).
 - ¹⁹V.L. Pokrovsky, J. Phys. (Paris) **42**, 761 (1981).
 - ²⁰C. Willis, M. El-Batanouny, and P. Stancioff, Phys. Rev. B **33**, 1904 (1986).
 - ²¹B. Joós and M.S. Duesbery, Phys. Rev. Lett. **78**, 266 (1997).
 - ²²J.F. Currie, S.E. Trullinger, A.R. Bishop, and J.A. Krumhansl, Phys. Rev. B **15**, 5567 (1977).
 - ²³R. Boesch and C.R. Willis, Phys. Rev. B **39**, 361 (1989).
 - ²⁴G.H. Vineyard, J. Phys. Chem. Solids **3**, 121 (1957).
 - ²⁵K.C. Pandey and E. Kaxiras, Phys. Rev. Lett. **66**, 915 (1991).
 - ²⁶M. Peyrard and M. Remoissenet, Phys. Rev. B **26**, 2886 (1982).
 - ²⁷V.V. Bulatov, S. Yip, and A.S. Argon, Philos. Mag. A **72**, 453 (1995).
 - ²⁸M.S. Duesbery, D.J. Michel, E. Kaxiras, and B. Joós, in *Defects in Materials*, edited by P. D. Bristowe, J.E. Epperson, J.E. Griffith, and Z. Liliental-Weber, MRS Symposia Proceedings No. 209 (Materials Research Society, Pittsburgh, 1991), p. 125.
 - ²⁹H. Alexander, in *Dislocations in Solids*, edited by F.R.N. Nabarro (North-Holland, Amsterdam, 1986), Vol. 7, p. 113.
 - ³⁰P.B. Hirsch, A. Ourmazd, and P. Pirouz, Inst. Phys. Conf. Ser. **60**, 29 (1981).
 - ³¹F. Louchet, Inst. Phys. Conf. Ser. **60**, 35 (1981).
 - ³²G. Schottky, Phys. Status Solidi **5**, 697 (1964).
 - ³³M.S. Duesbery, Acta Metall. **31**, 1747 (1983).
 - ³⁴T.A. Parthasarathy, S.I. Rao, and D.M. Dimiduk, Philos. Mag. A **67**, 643 (1993).
 - ³⁵S.I. Rao, T.A. Parthasarathy, M.S. Duesbery, and D.M. Dimiduk (private communication).